Giornate di Studio SPARX e Applicazioni
INFN-LNF, Frascati, 9-10 May 2005

Image reconstruction of non periodic nanostructured objects using coherent X-ray diffraction (CXD)

Campi G., De Caro L., Giannini C., Guagliardi A., Margonelli A., Pifferi A.

Istituto di Cristallografia
Crystallography Institute

INTRODUCTION

- Why coherent X ray diffraction (CXD)?

THE CXD TECHNIQUE

- Limits on the experimental setup arising from coherent scattering from non periodic objects
- Phasing of diffuse scattering: image reconstruction

APPLICATIONS

- Examples of image reconstruction from CXD
- Our plans, new experiments: CNXD

LIMITATIONS AND PERSPECTIVES

- Dose and flux limitations
- Femtosecond CXD

INTRODUCTION

Can the beam coherence and intensity produce the crystal amplification effect (also without a periodic object arrangement)?

D. Sayre "*Imaging Processes and Coherence in Physics*"
in Lecture Notes in Physics, Vol. 112, pp. 229-235 (1980)

nano-materials: assembly of inorganic, organic, biological nanostructures

3° generation synchrotron sources ⇒ Res = 7 nm ⇒ Crystallography… without crystals?

J. Miao et al.,
Phys. Rev. B **67**, 174104 (2003)

CXD: imaging non periodic objects with larger thickness in comparison with Scanning probe methods and Electron microscopy

THE CXD TECHNIQUE

2) Sampling: recording is made of an oversampled diffraction pattern

1) Coherence: the sample is illuminated by monochromatic coherent x-rays

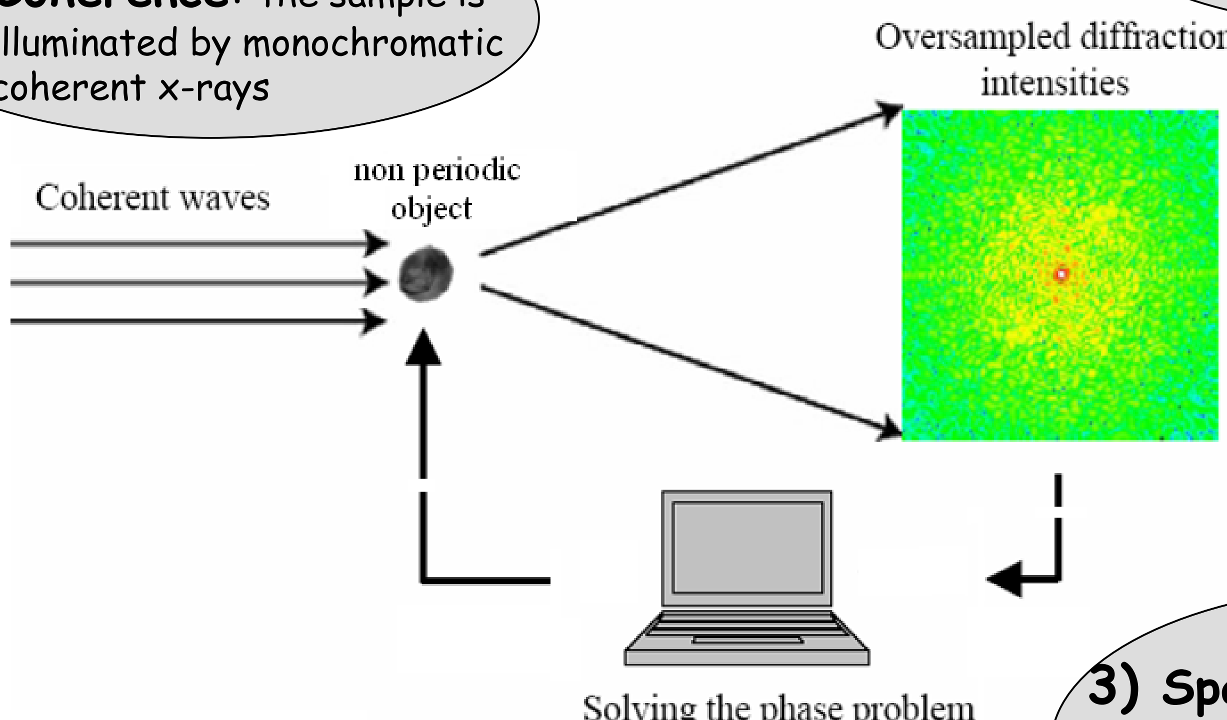

3) Spatial and temporal beam coherence: the sampling is correlated with the beam coherence

4) Image reconstruction: phasing diffuse scattering

Coherence

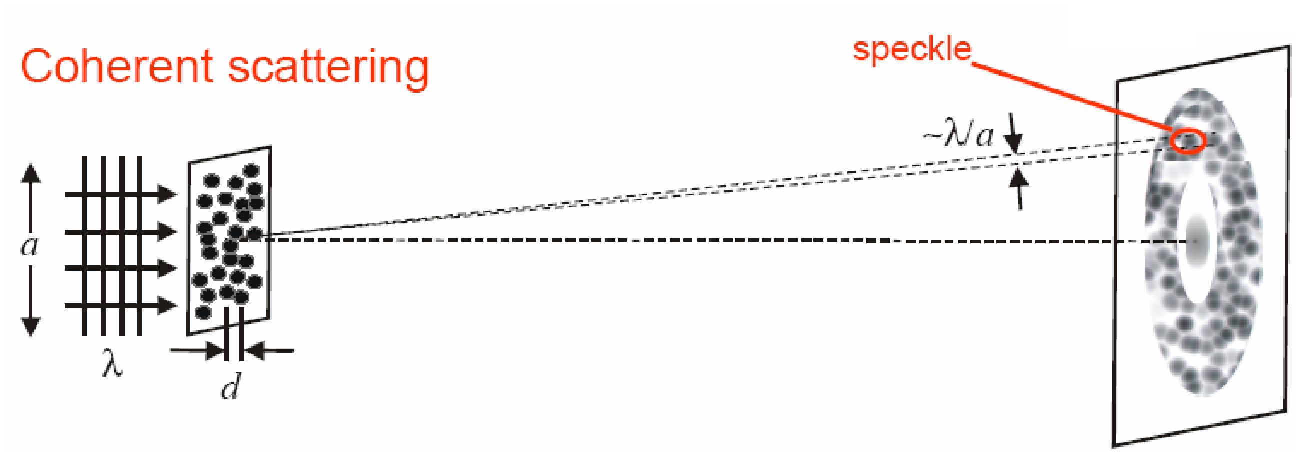

Result of an interference process of the beams diffracted from each single object.
The typical `speckle' pattern contains the spatial information on the single scattering object.

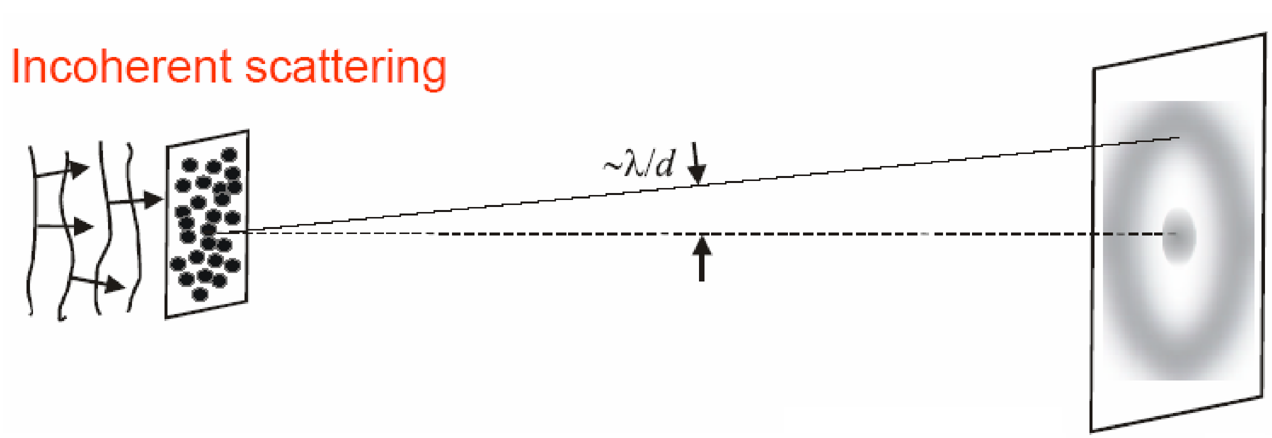

Result that resembles an average over an ensemble of slightly different particle configuration, over particle distances.

Sampling

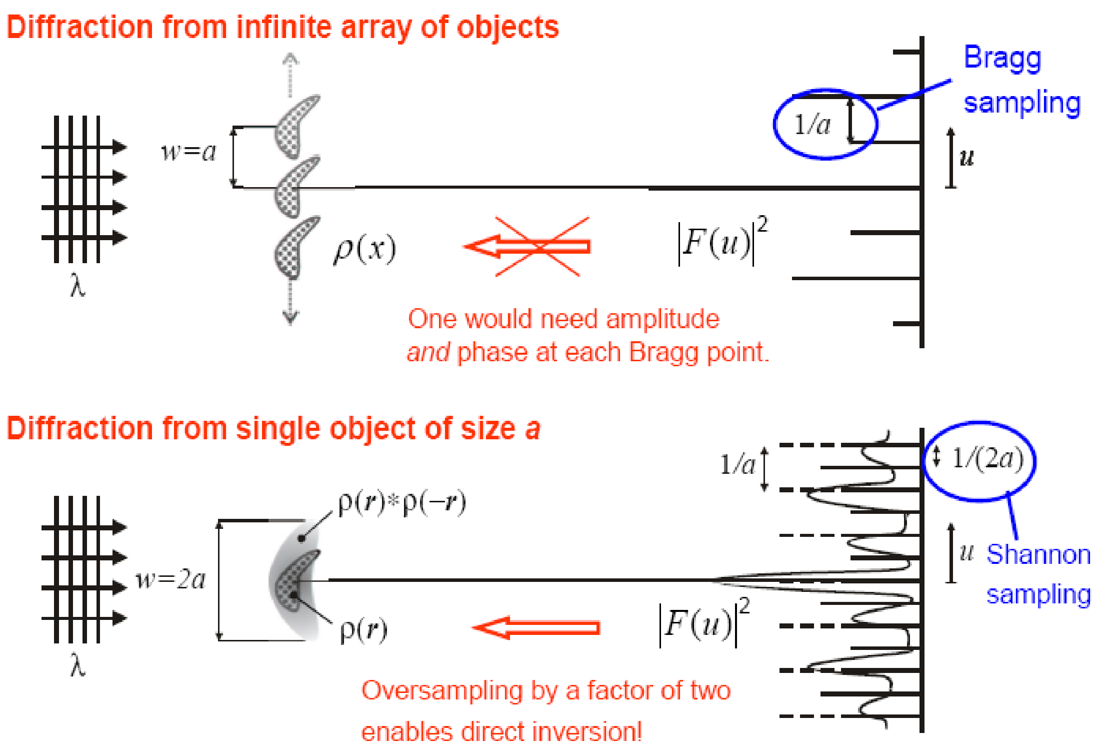

The Shannon interval for frequency-space sampling of the intensity is

$$\Delta S < \frac{1}{2a}$$

This corresponds to surrounding the electron density of the sample with a no-density region; generally, we can define the oversampling ratio as

$$O = \frac{A(\rho > 0) + A(\rho = 0)}{A(\rho > 0)}$$

Spatial and temporal beam coherence

The oversampling method is strongly correlated with the coherence of the incident x rays.

Temporal (longitudinal) coherence

(degree to which waves have a well defined phase).

$$\xi_l \simeq \frac{\lambda^2}{2\Delta\lambda}$$

→ $\xi_l > PLD_{max}$

$PLD_{max} \sim q_{max} \sim 1/Res$

→

$$\frac{\lambda}{\Delta\lambda} \geq \frac{Oa}{Res}$$

where $Res = \lambda/2\sin\theta_{max}$

Spatial (transverse) coherence

(degree to which wave front has a well defined phase)

Sampling at $\Delta S \sim 1/Oa$ corresponds to an angular pixel size of $\Delta\alpha = \lambda/Oa$ which the detector must resolve and so:

$$\Delta\theta \leq \frac{\lambda}{Oa}$$

→

$$Oa \leq \frac{\lambda}{\Delta\theta} = \xi_t$$

→

The higher the oversampling degree, the finer the sampling of the diffraction pattern has to be, and hence the larger the coherence length of the incident beam needs to be.

Other useful setting parameters and devices:

The sample-detector distance (L)

$$\Delta\theta \leq \frac{\lambda}{Oa} \Longrightarrow L \sim \frac{d_{pix} a}{\lambda} O$$

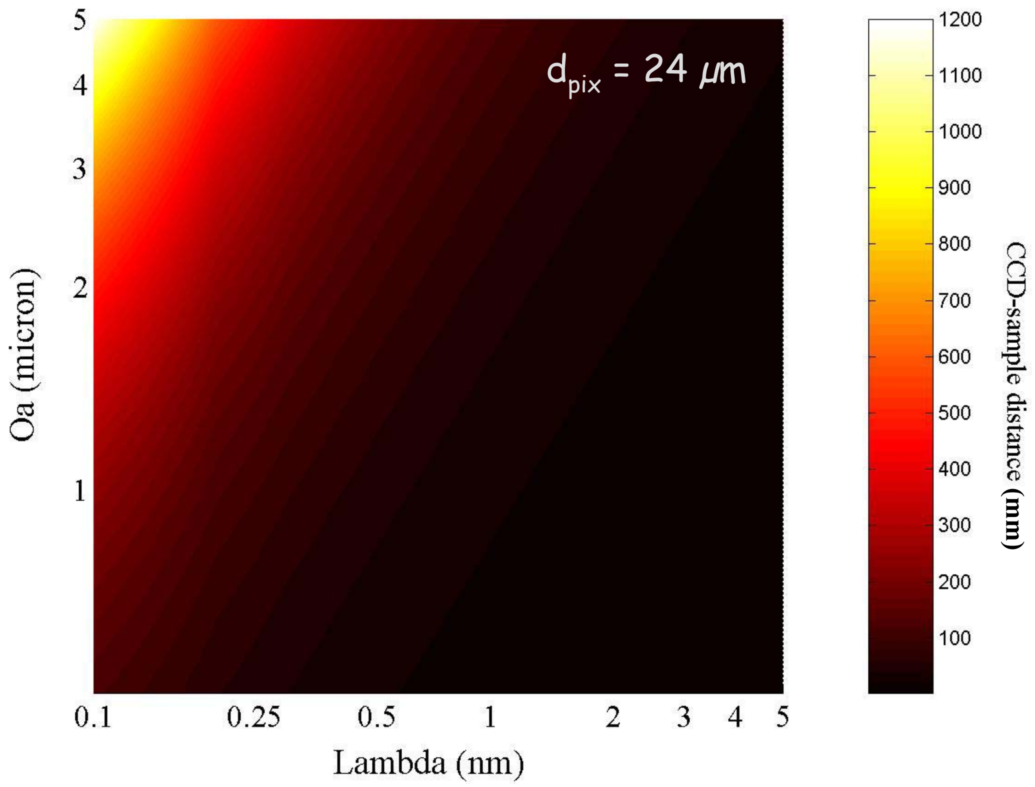

Pinholes and slits

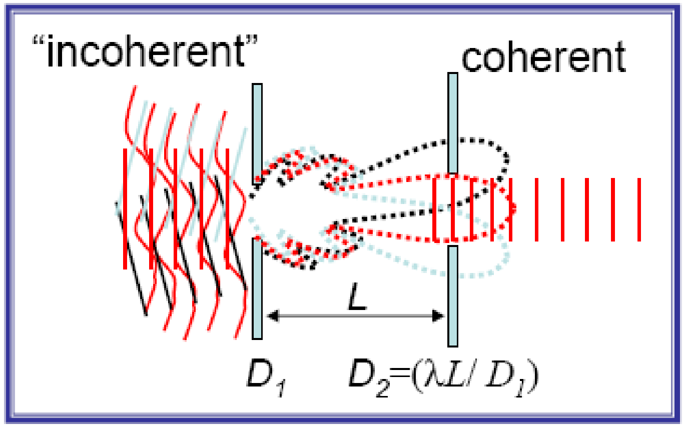

Image reconstruction:
phasing of diffuse scattering

Fienup *HiO* algorithm
(Fienup, 1982, 1987)

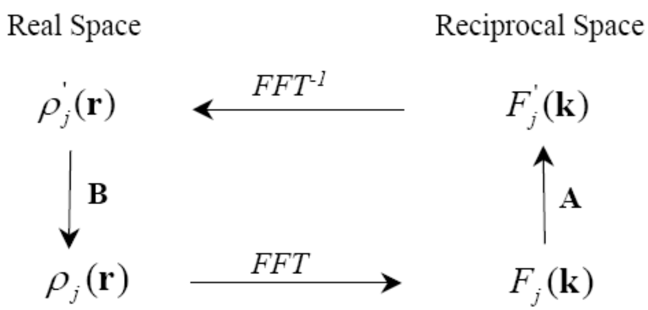

A: $$F_j'(\mathbf{k}) = \left|F_{\exp}(\mathbf{k})\right| \times e^{\varphi_{j-1}(\mathbf{k})}$$

B: $$\rho_j(\mathbf{r}) = \begin{cases} \rho_j'(\mathbf{r}) & if\ \mathbf{r} \in S \cap \rho_j'(\mathbf{r}) \geq 0 \\ \rho_{j-1}(\mathbf{r}) - \beta \times \rho_j'(\mathbf{r}) & if\ \mathbf{r} \notin S \cup \rho_j'(\mathbf{r}) < 0 \end{cases}$$

The algorithm iterated back and forth between real and reciprocal space with a random phase set as the initial input. **In real space, B, a finite support has to be defined to separate the electron density and the no-density regions.**

Modified *direct methods*
(Spence et al., 2003;
Carrozzini et al.,2004)

We search for a more general phasing procedure, based on

- no use of any support, such as masks based on the autocorrelation function or SEM images.
- no prior knowledge of the scattering factor of particles or of their number.

APPLICATIONS

State of the art

by

…3 significant experiments……

The first demonstration experiment

Recording diffraction patterns from noncrystalline specimens:
Au dots (100nm in diameter, 80nm in thick) on a silicon nitride membrane

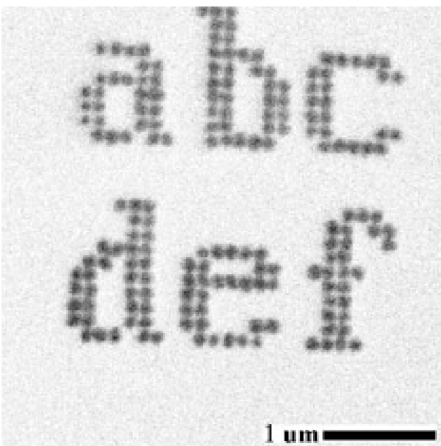

(a) SEM image of a layered sample

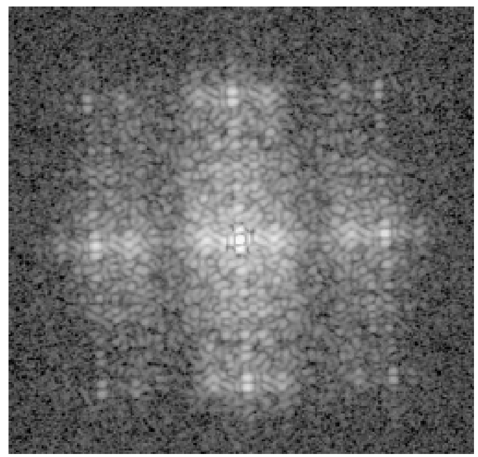

(b) Coherent diffraction pattern from (a)

(c) Reconstructed image from (b)

To make a small clean beam:
a 20-μm pinhole placed at 25 mm upstream of the sample.

λ = 1.7 nm
N_{pix} = 512
d_{pix} = 24 μm
L = 250 mm

Oa ~60 μm
Res = 75 nm

Miao *et al.*, Nature 400, 342 (1999)

Our reconstruction method: the modified SIR2002 program

non-periodic array of gold balls of 50 nm diameter


SEM image

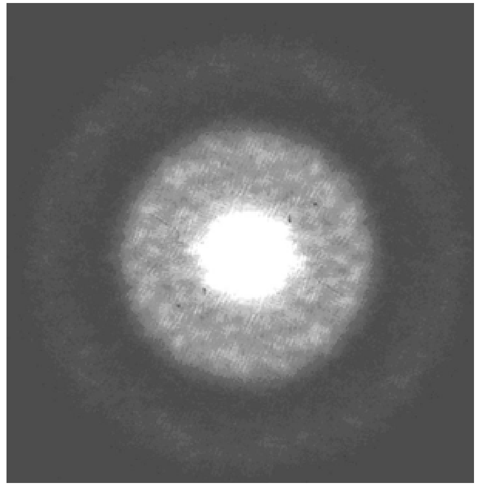
Soft X-ray transmission diffraction pattern

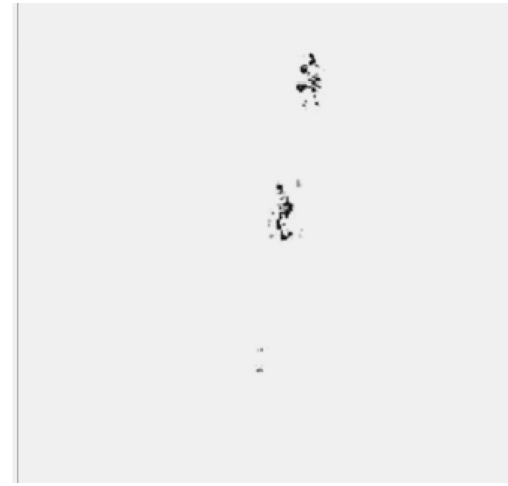
Recovered charge density

To make a small clean beam:
a 5-μm pinhole placed at 25 mm upstream of the sample.

λ = 2.11 nm

N_{pix} = 1025

d_{pix} = 25 μm

L = 110 mm

Oa ~ 10 μm

Res ~ 50 nm

B. Carrozzini et al., Acta Cryst. A60, 331, (2004)

Imaging biological samples

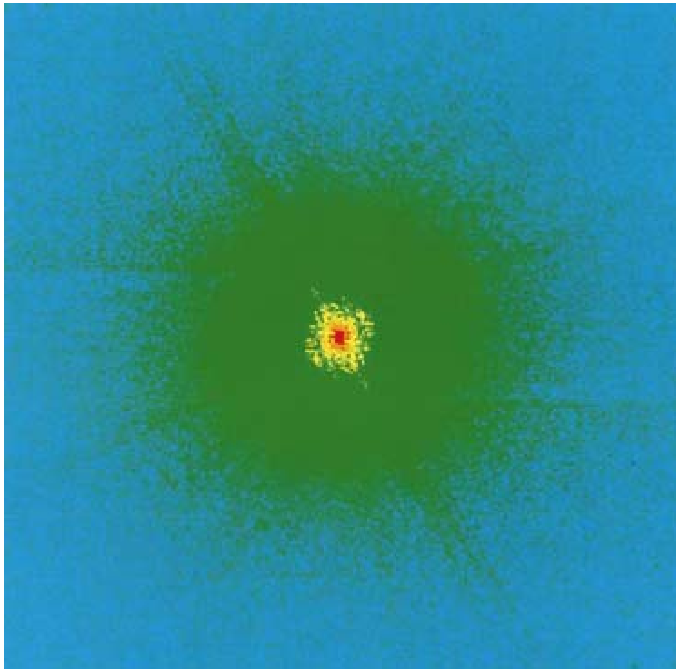

(A) diffraction pattern from *E. coli* bacteria displayed in a logarithmic scale.

Beam divergence: $6 \cdot 10^{-6}$ rad
by setting a 150-mm pinhole at a distance of 27 m upstream of the experimental instrument
(at undulator beamline at SPring-8)

CCD-sample distance: 743 mm
x-rays wavelength: 2Å
Res: 30 nm

To make a small clean beam:
a 20-μm pinhole and a corner slit placed at 25.4 and 12.7 mm upstream of the sample.

(B) An image reconstructed from (A)

The dense regions inside the bacteria are likely the distribution of proteins labeled with KMnO4.

The semi transparent regions are devoid of proteins.

Miao *et al.*, *Proc. Natl. Acad. Sci. USA* **100**, 110 (2003)

OUR PLANS, NEW EXPERIMENTS:

…..what can we do with CXD & FEL-SPARX?

…we have seen limits:

Pin holes and slits: coherence degree…
…not so good

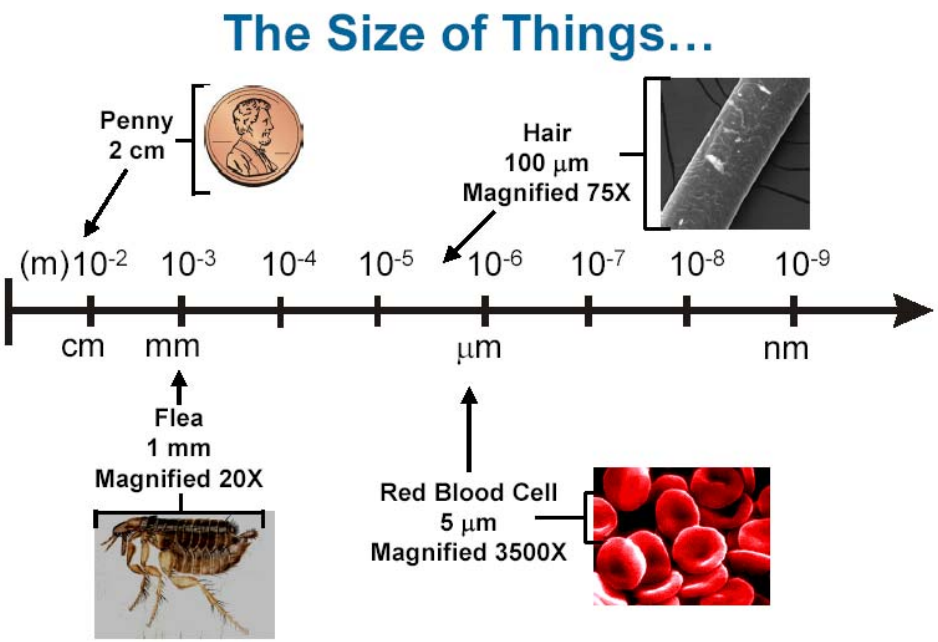

Oa > 1 μm

The SPARX source provides a beam already temporarily and spatially coherent at the micrometric scale (support dimension)

but…
if we move at a nanometric scale…

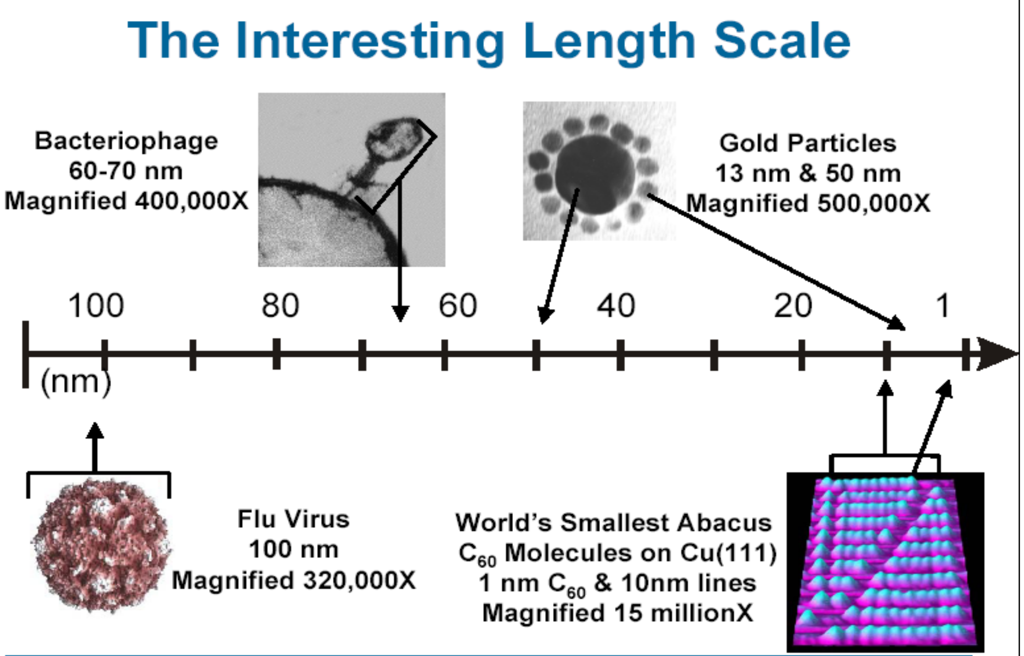

nano-materials: assembly of inorganic, organic, biological nanostructures

We need ***coherent*** x-ray ***nano***-beams!

And so...

we propose to use **array of 2D Waveguides** at **SPARX**

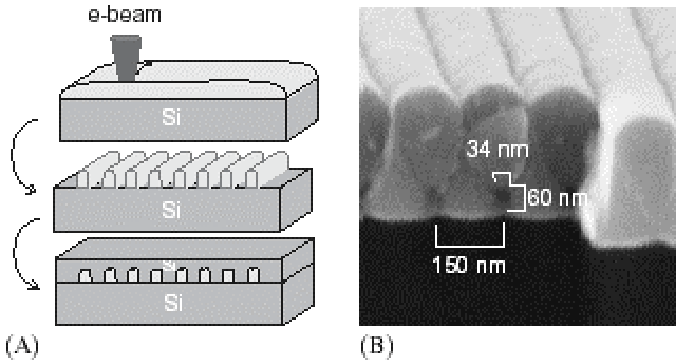

Fig. 1. (A) Sketch of the fabrication process. (B) Scanning electron micrograph (SEM) of the calixarene grating after evaporation of silicon.

Arrays of 2D waveguide nanostructures have been fabricated by e-beam lithography.

•the area coherently illuminated is reduced

•the coherence degree is preserved with respect to pinholes or slits

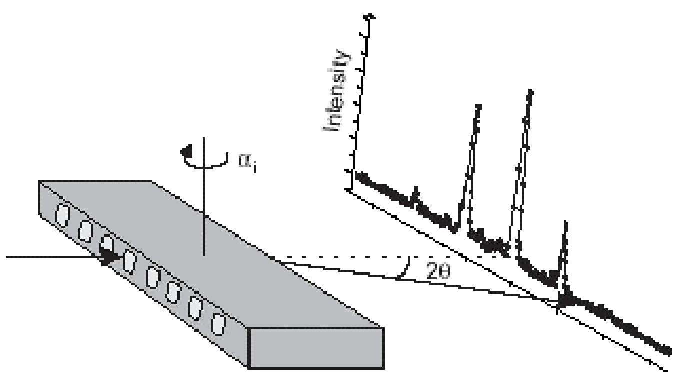

Fig. 2. Sketch of the experimental setup used to measure the far-field pattern of the waveguide grating.

❖Angular divergence (~N)

❖Intensity (~N^2)

Ollinger et al., *Physica B* ***357***, *53 (2005)*

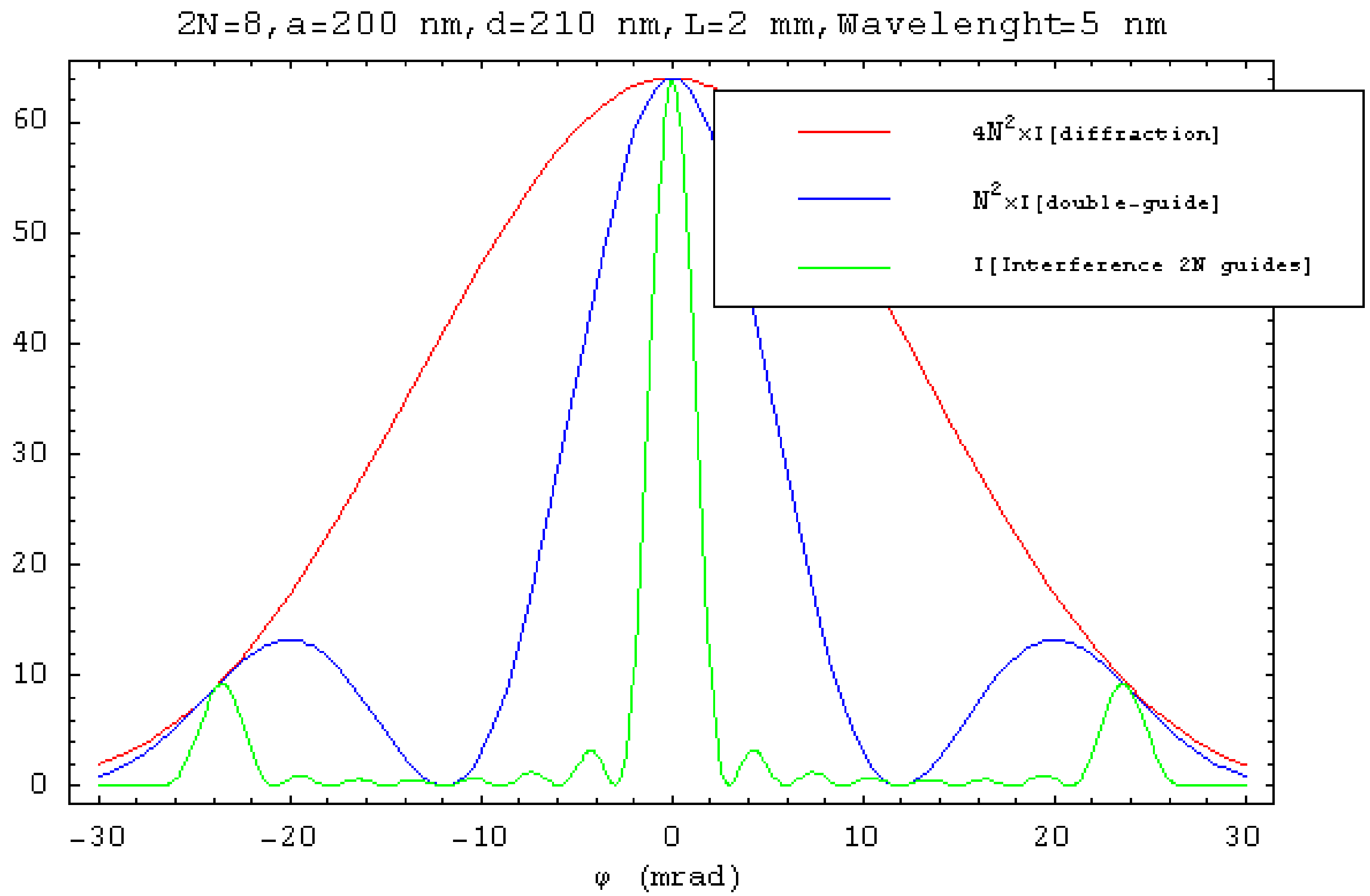

❖We can control the interference peaks by a_{WG}, d_{WG}:

- $d_{WG} \sim a_{WG}$

$$\Delta\theta \leq \frac{\lambda}{2Oa}$$

Oversampling condition

Experimental conditions

Far-field condition

$$L2 \geq \frac{(Oa)^2}{\lambda}$$

Given *Oa*, λ ::>> the minimum value for sample to CCD distance **L2** is defined

Overlapping condition

It defines the minumum value for WG to sample distance **L1**

$$L1 \geq \frac{(2N-1)^2 d^2}{\lambda}$$

the number of waveguides (2N) is given by

$$\Delta\theta_N \approx \frac{\lambda}{N(2d + a_{WG})} \approx \frac{\lambda}{3Na_{WG}} \leq \frac{\lambda}{2Oa}$$

+

$$\lambda L2 = d_{pix} Oa$$

It fixes the CCD pixel size

…for example…

Support:

$Oa = 1\mu m$

→

WG array:

$a_{WG} \sim d = 200nm$

$N \sim 7$

CCD:

$d_{pix} = 80\ \mu m$

$N_{pix} = 1024$

Wavelength: $\lambda = 5nm$

$L2 \geq 16$ mm

$L1 \geq 1.35$ mm

$\Delta\theta \leq 2.5$ mrad

$Res \geq 2.7$ nm

Wavelength: $\lambda = 1\ nm$

$L2 \geq 80$ mm

$L1 \geq 6.76$ mm

$\Delta\theta \leq 0.5$ mrad

$Res \geq 1.1$ nm

LIMITATIONS AND PERSPECTIVES

One of the main challenges in CXD is to improve resolution, but, dose and flux limitations arise: Radiation damage

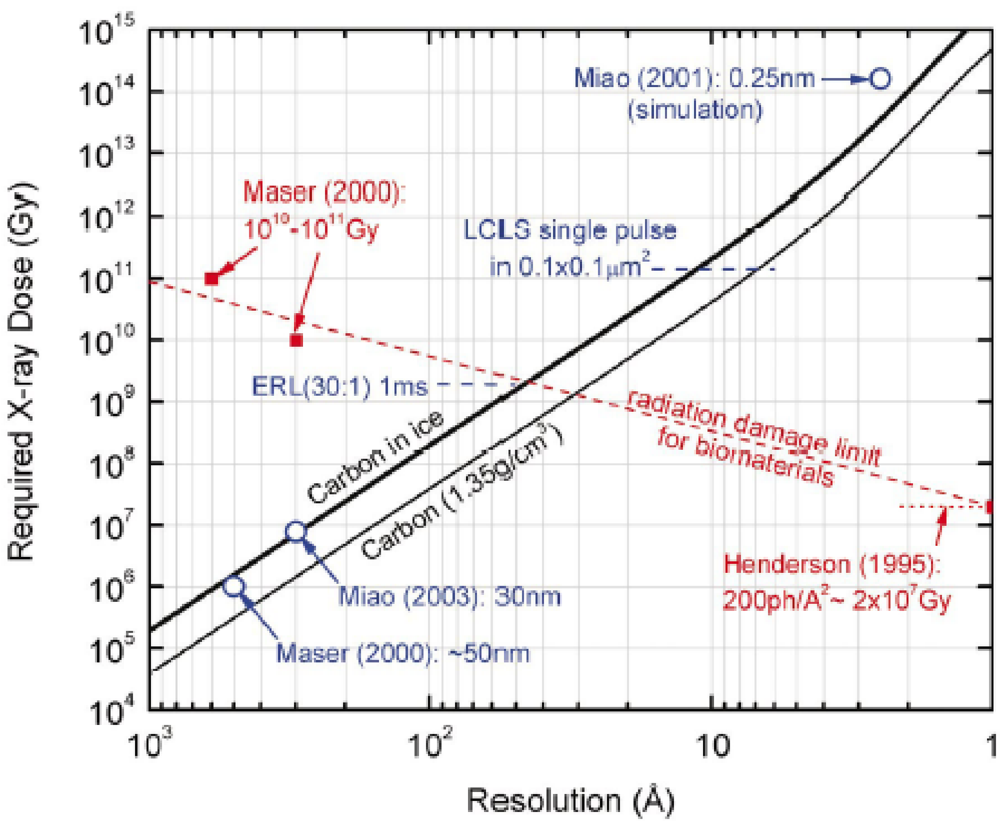

Shen et al., J. Synch. Rad **11**, 432 (2004)

Femtosecond CXD: beyond the radiation-damage limit

With an X-FEL of pulse leng. < 50 fs and 3 x 10^{12} photons focused down to a spot of ~ 0.1 μm, a 2D diffraction pattern could be recorded from a biomolecule before the radiation damage manifests itself.

S. Solemn et al., *Science* 218, 229 (1982)
N. Neutze et al., *Nature* 400, 752 (2000)

in summary…

- **CXD** provides a new imaging methodology by combining coherent X-rays with the oversampling method.

- **CNXD** is possible with FEL-SPARX source and arrays of waveguides